Supplementary Information

In situ growth of heterojunction cocatalyst on g-C_3N_5 surface enhances charge transfer to improve photocatalytic activity
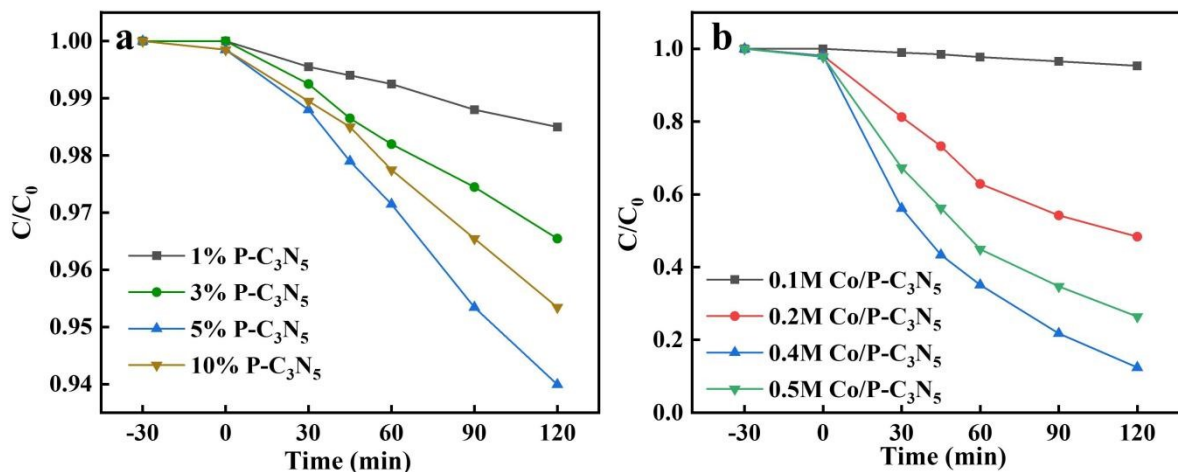

Figure.S1. (a)Photocatalytic degradation of TC under visible light (30 min in the dark) by different P contents of P-C_3N_5, and (b) by different Co contents of CoOOH·CoO$_x$/P-C_3N_5
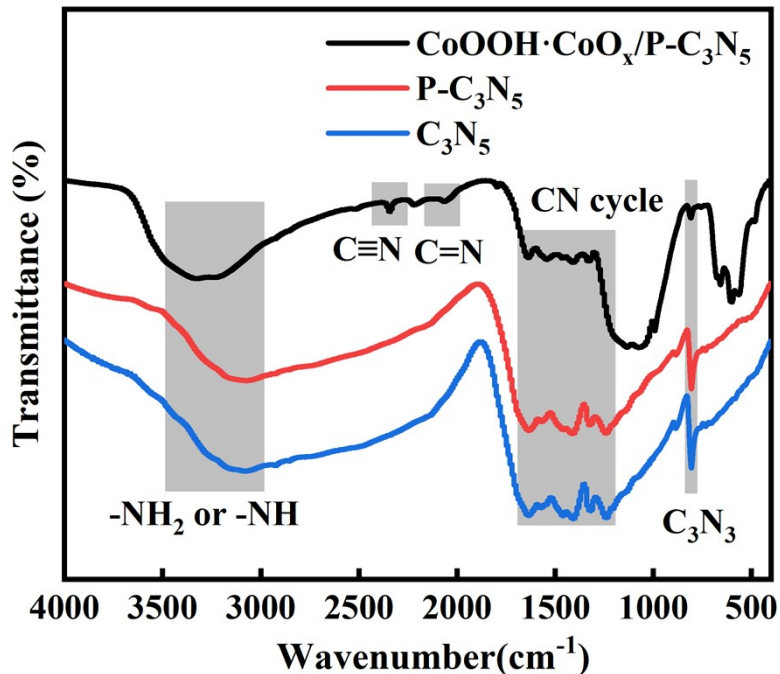

Figure.S2. FTIR of C_3N_5, P-C_3N_5 and CoOOH·CoO$_x$/P-C_3N_5
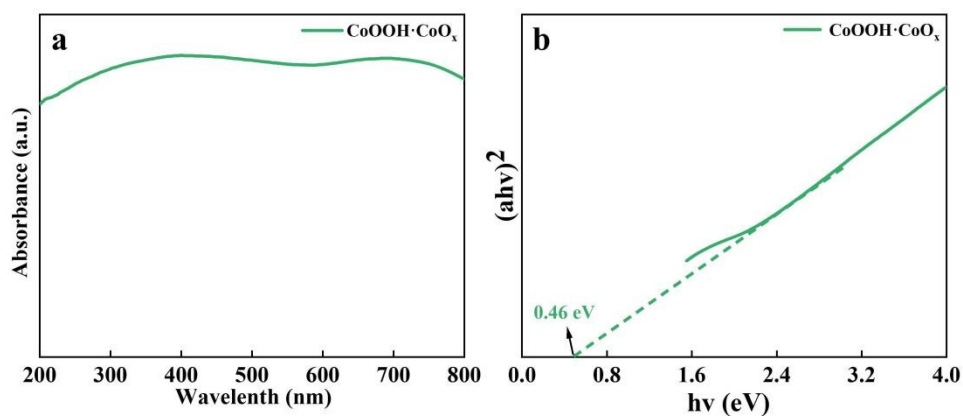
Figure. S3.(a) UV-vis absorption spectra and (b) (ahv)^2 versus hv curves of the CoOOH·CoO$_x$.
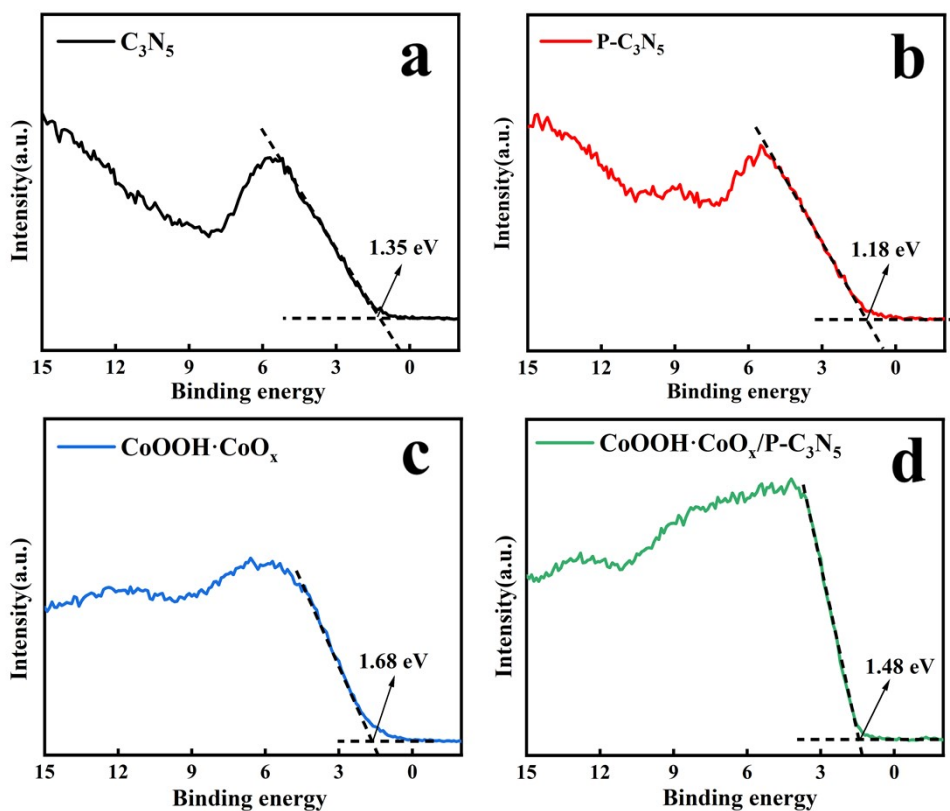
Figure. S4. XPS Vb of (a)C$_3$N$_5$, (b)P-C$_3$N$_5$, (c)CoOOH·CoOx and (d)CoOOH·CoO$_x$/P-C$_3$N$_5$

As shown in Figure S3 and Figure S4, the CoOOH·CoO$_x$ in these figures is not in-situ growth on the surface of P-C$_3$N$_5$, which may be different from the CoOOH·CoO$_x$ in the proposed material, but it is still of certain reference value.
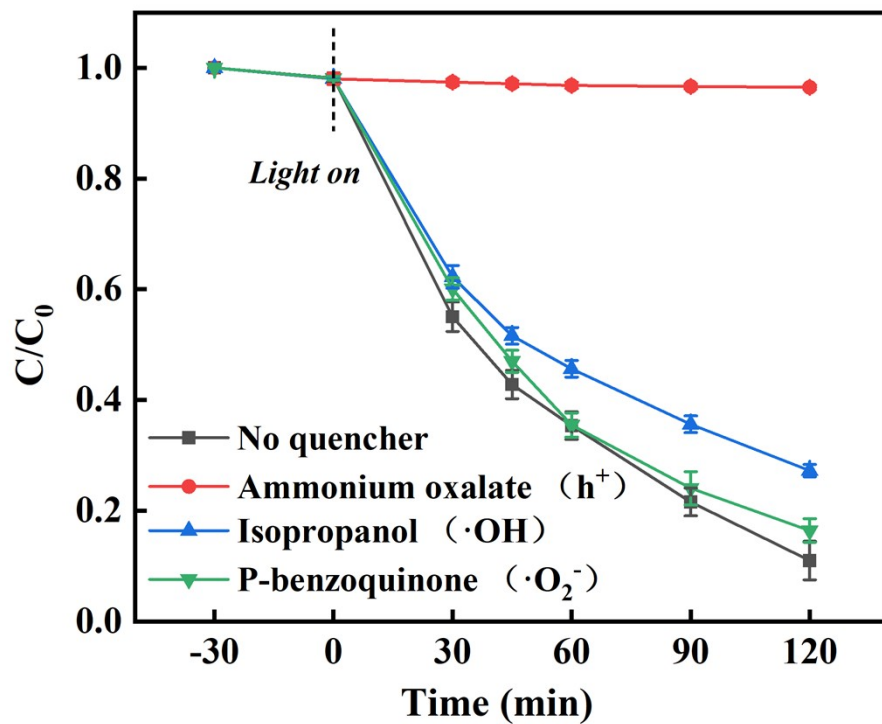
Figure.S5. Masking experiment of TC degradation by $CoOOH \cdot CoO_x/P-C_3N_5$

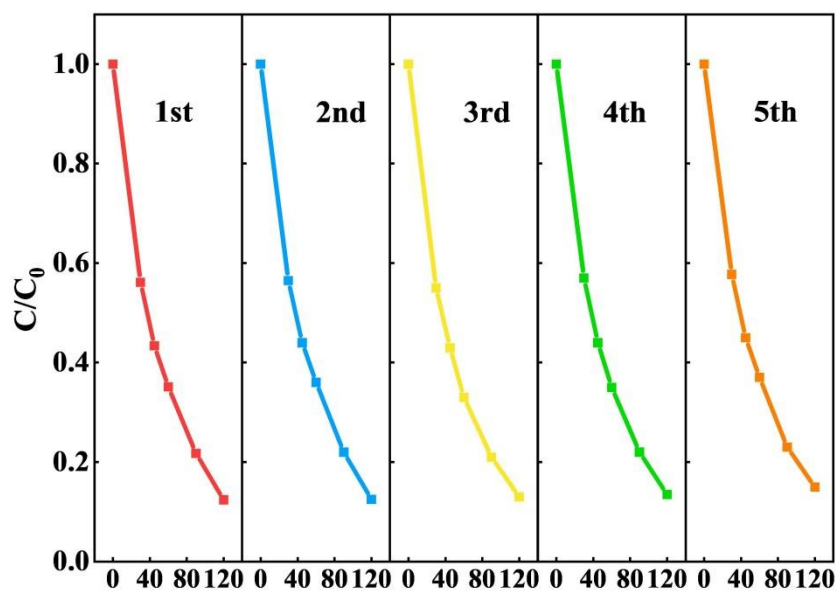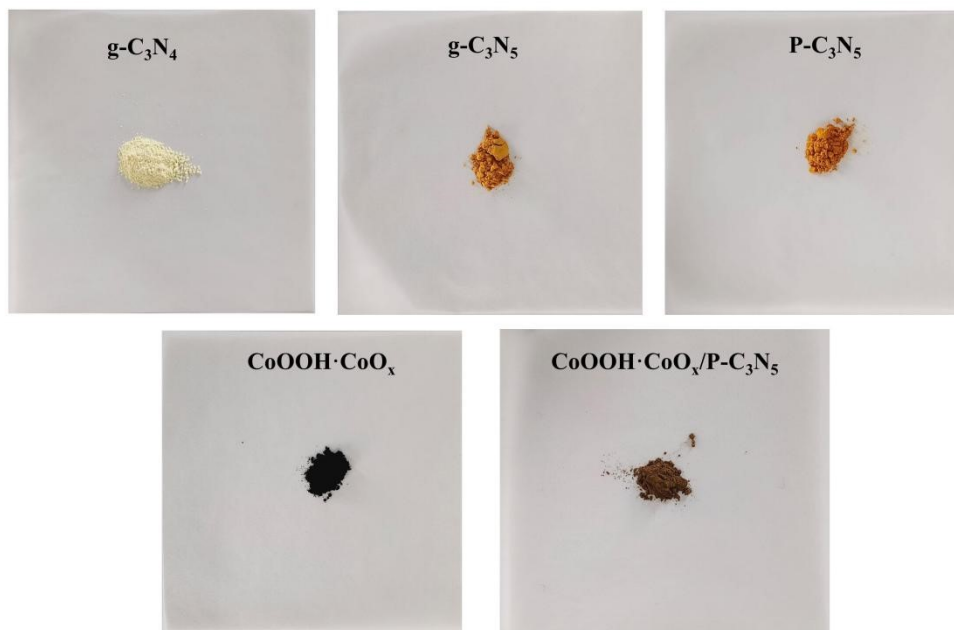Figure.S6. Cyclic experiment of TC degradation by $CoOOH \cdot CoO_x/P-C_3N_5$

Figure.S7. Photos of g-C$_3$N$_4$, g-C$_3$N$_5$, P-C$_3$N$_5$, CoOOH·CoO$_x$ and CoOOH·CoO$_x$/P-C$_3$N$_5$
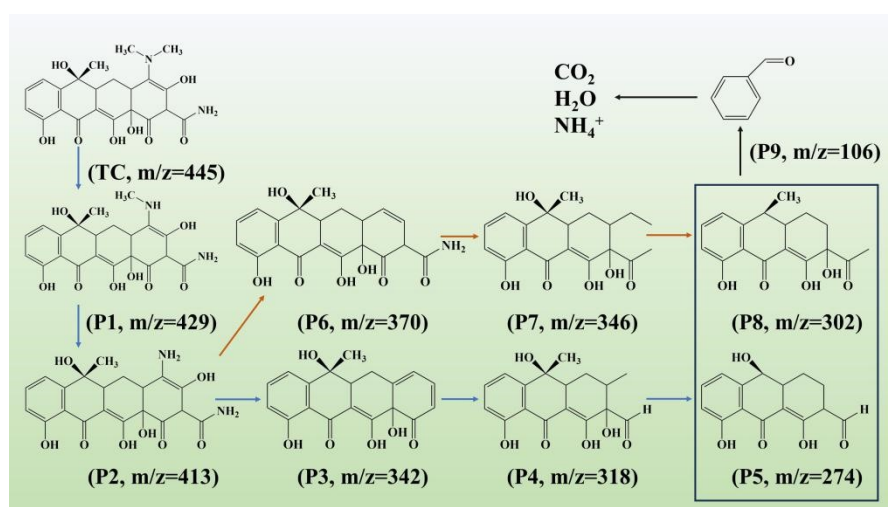

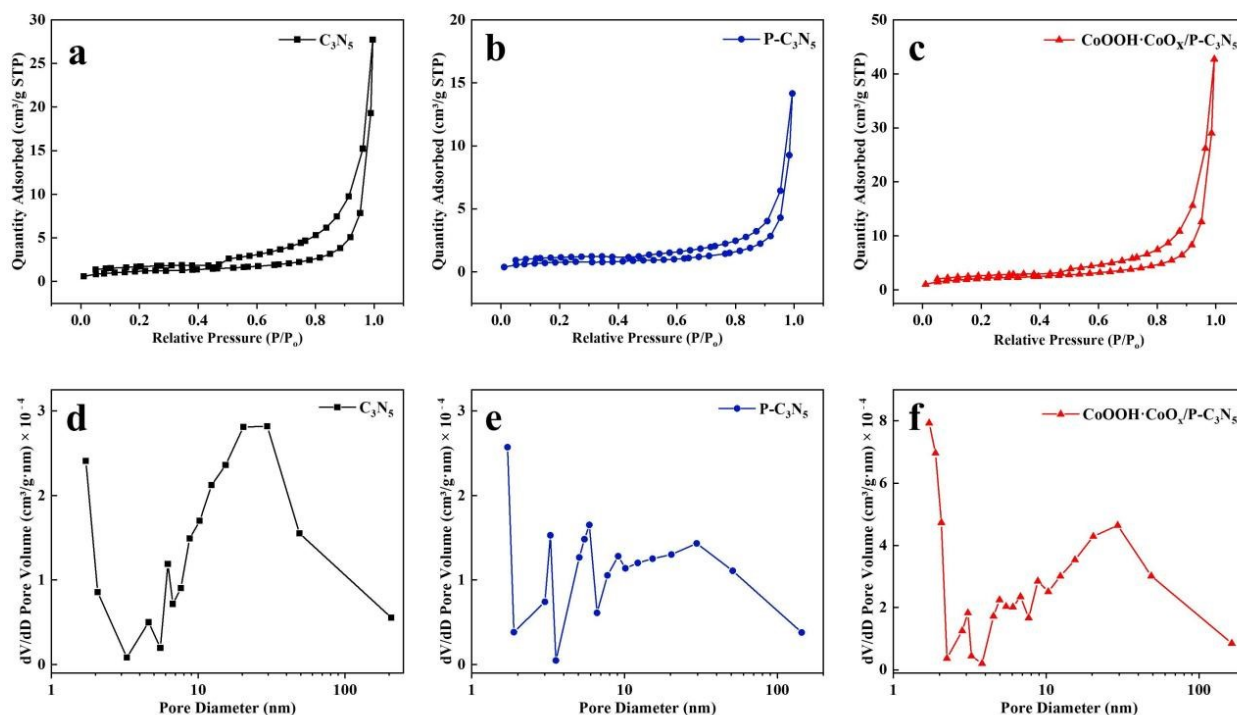Figure.S8. The proposed photocatalytic-degradation pathways of TC

Figure.S9. N_2 adsorption–desorption isotherms of C_3N_5 (a), P-C_3N_5 (b) and CoOOH·CoO$_x$/P-C_3N_5 (c), the pore-size distribution curves for C_3N_5 (d), P-C_3N_5 (e) and CoOOH·CoO$_x$/P-C_3N_5 (f).

As shown in Fig. S9, nitrogen adsorption–desorption is used to investigate the pore structure and surface areas of C_3N_5, P-C_3N_5 and CoOOH·CoO$_x$/P-C_3N_5. All the samples display type IV curves, indicating the presence of mesopores [1]. The shape of the hysteresis loops for the three samples is categorized as type H3, which implies the formation of slit-like pores owing to the aggregation of the sheet-like particles [1]. The CoOOH·CoO$_x$/P-C_3N_5 sample contains small mesopores (3–4 nm) and large mesopores (20–50 nm). As shown in Table S1, the BET surface areas (S_{BET}) and pore volume of CoOOH·CoO$_x$/P-C_3N_5 are the highest, which is consistent with the results of SEM. This mesoporous hierarchical architecture could provide a transport path for the reactants and products and offers more active sites and enhance photo-energy harvesting in photocatalysis [1–4].

Table S1. Summary of the S_{BET}, pore volume, and peak pore size.

Samples	$S_{BET}(m^2 / g)$	Pore volume (cm^3 / g)	Peak pore size (nm)
C_3N_5	4.3	0.043	6.4/23.5
P-C_3N_5	2.8	0.022	5.9/27.3
CoOOH·CoO$_x$/P-C_3N_5	7.6	0.066	8.6/29.6

Reference

[1] J. Zhang, J. Yu, Y. Zhang, Q. Li, J.R. Gong, Visible Light Photocatalytic H_2-Production Activity of CuS/ZnS Porous Nanosheets Based on Photoinduced Interfacial Charge Transfer, Nano Lett. 11 (2011) 4774–4779. https://doi.org/10.1021/nl202587b.

[2] G. Li, D. Zhang, J.C. Yu, M.K.H. Leung, An Efficient Bismuth Tungstate Visible-Light-Driven Photocatalyst for Breaking Down Nitric Oxide, Environ. Sci. Technol. 44 (2010) 4276–4281. https://doi.org/10.1021/es100084a.

[3] X. Yu, J. Yu, B. Cheng, M. Jaroniec, Synthesis of Hierarchical Flower-like AlOOH and TiO_2/AlOOH Superstructures and their Enhanced Photocatalytic Properties, J. Phys. Chem. C 113 (2009) 17527–17535. https://doi.org/10.1021/jp906992r.

[4] W. Shao, F. Gu, L. Gai, C. Li, Planar scattering from hierarchical anatase TiO_2 nanoplates with variable shells to improve light harvesting in dye-sensitized solar cells, Chem. Commun. 47 (2011) 5046. https://doi.org/10.1039/c1cc10548e.